Original Article

Parabanic acid is the singlet oxygen specific oxidation product of uric acid

Sayaka Iida, Yuki Ohkubo, Yorihiro Yamamoto and Akio Fujisawa*

School of Bioscience and Biotechnology, Tokyo University of Technology, 1404-1 Katakura-cho, Hachioji, Tokyo 192-0982, Japan

(Received 8 March, 2017; Accepted 16 May, 2017; Published online 5 September, 2017)

Uric acid quenches singlet oxygen physically or reacts with it, but the oxidation product has not been previously characterized. The present study determined that the product is parabanic acid, which was confirmed by LC/TOFMS analysis. Parabanic acid was stable at acidic pH (<5.0), but hydrolyzed to oxaluric acid at neutral or alkaline pH. The total yields of parabanic acid and oxaluric acid based on consumed uric acid were ~100% in clean singlet oxygen production systems such as UVA irradiation of Rose Bengal and thermal decomposition of 3-(1,4-dihydro-1,4-epidioxy-4-methyl-1-naphthyl)propionic acid. However, the ratio of the amount of uric acid consumed to the total amount of singlet oxygen generated was less than 1/180, indicating that most of the singlet oxygen was physically quenched. The total yields of parabanic acid and oxaluric acid were high in the uric acid oxidation systems with hydrogen peroxide plus hypochlorite or peroxynitrite. They became less than a few percent in peroxyl radical-, hypochlorite- or peroxynitrite-induced oxidation of uric acid. These results suggest that parabanic acid could be an *in vivo* probe of singlet oxygen formation because of the wide distribution of uric acid in human tissues and extracellular spaces. In fact, sunlight exposure significantly increased human skin levels of parabanic acid.

***Key Words*: singlet oxygen, uric acid, parabanic acid, oxaluric acid, sunlight exposure**

Oxidative stress induces lipid peroxidation,[1] DNA damage,[2] and protein carbonylation,[3] which can lead to diseases such as cancer,[4] diabetes,[5] Alzheimer's disease,[6] and ischemia reperfusion injury.[7,8] Since initial oxidative stress is caused by various reactive oxygen species (ROS), the importance of identifying ROS *in vivo* is of interest in clinical investigations.

Identifying ROS *in vivo* can be done by monitoring an oxidation product as a marker. The oxidized substrate must show high reactivity toward different ROS and yield a specific oxidation product from an individual ROS. Uric acid (UA, Fig. 1) is an adequate substrate for this purpose. Uric acid is a terminal metabolite of purine in primates including humans. It is also a water-soluble antioxidant that can scavenge many types of ROS: free radicals,[9] peroxynitrite ($ONOO^-$),[10] hypochlorous anion (ClO^-),[11] and singlet oxygen ($^1O_2$).[9] Furthermore, its oxidation products are specific to the ROS (Fig. 1): free radical-induced oxidation gives allantoin (AL);[12] $ONOO^-$-induced oxidation yields triuret;[13] and nitric oxide ($^{\bullet}NO$) gives 6-aminouracil.[14] However, the $^1O_2$ induced-oxidation product has not been identified.

Singlet oxygen ($^1O_2$) is a prominent ROS that plays an important role in bactericidal action. Nakano *et al.*[15] showed that $^1O_2$ killed *E. coli* effectively, although it was not harmful against human umbilical vein endothelial cells. Because the respiratory chains of eukaryotic cells are enclosed in mitochondria, whereas those of prokaryotic cells are contained in the cell membrane, $^1O_2$ penetrating from the cell surface turns into harmless triplet molecular oxygen ($^3O_2$) before it reaches the mitochondria. Therefore, $^1O_2$ can be considered a relatively innocuous ROS against eukaryotic cells. However, an excess amount of $^1O_2$ can damage organisms, and some reports indicate that it causes oxidative damage to lipids,[16] proteins,[17] and DNA,[18] and also induces apoptosis.[19] Photosensitization is usually used to produce $^1O_2$, but two-electron oxidation of H_2O_2 also can generate $^1O_2$.[20] The oxidation of H_2O_2 mimics myeloperoxidase (MPO), which produces ClO^- from H_2O_2 and Cl^-. The ClO^- anion is a strong oxidant that can oxidize H_2O_2 to $^1O_2$, [21] which suggests that $^1O_2$ production may occur *in vivo* without sunlight exposure.

The current study demonstrated that parabanic acid (PA, Fig. 1) was formed specifically by $^1O_2$-induced UA oxidation. Production of $^1O_2$ resulted from thermal decomposition of 3-(1,4-dihydro-1,4-epidioxy-4-methyl-1-naphthyl)propionic acid (NEPO), photooxidation using Rose Bengal, and H_2O_2 oxidation by ClO^- or $ONOO^-$, and PA was produced in high yield. However, the yield of PA was less than a few percent from peroxyl radical-, ClO^-- or $ONOO^-$-induced oxidation of UA. These results strongly suggest that PA is an oxidation product specific to $^1O_2$ oxidation, and that PA and its hydrolysis product, oxaluric acid (OUA, Fig. 1), are suitable indicators of $^1O_2$ production *in vivo*.

Materials and Methods

Chemicals. UA, PA, and other chemicals were purchased from Wako Pure Chemical Industries, Co., Ltd. (Osaka, Japan), Tokyo Chemical Industry Co., Ltd. (Tokyo, Japan), or Waken B Tech Co, Ltd. (Kyoto, Japan), and used as received. An $ONOO^-$ generator, 3-(4-morpholinyl)sydnonimine hydrochloride (SIN-1), was purchased from Dojindo (Kumamoto, Japan). Authentic standard solutions of UA and PA were dissolved in 100 mM phosphate buffer (pH 7.4) and methanol, respectively, and stored at 4°C until use. The OUA was prepared by hydrolysis of PA upon addition of aqueous NH_3 and then the solution was neutralized using 1 M HCl. The OUA formation was confirmed by LC/time-of-flight mass spectrometry (TOFMS) analysis using an ion corresponding to OUA ($m/z = -131$) and its fragment ion ($m/z = -59$).

$ONOO^-$ was synthesized using a modified procedure described by Kato *et al.*[22] Briefly, an ice-cold 0.7 M H_2O_2 solution containing 0.6 M HCl (10 ml) was added to a well-stirred 0.6 M $NaNO_2$ solution (10 ml) in an ice bath, immediately followed by addition of 1.5 M NaOH (20 ml). The excess H_2O_2 was removed by addition of MnO_2. The solution was then frozen at –25°C. The $ONOO^-$ formed a yellow top layer due to frozen fractionation. This layer was collected and its concentration was determined as 330 mM by measuring its UV absorbance at 302 nm ($\varepsilon = 1{,}670\ M^{-1}\cdot cm^{-1}$).

*To whom correspondence should be addressed.
E-mail: afujisawa@stf.teu.ac.jp

doi: 10.3164/jcbn.17-24

Oxidation of UA with $^1O_2$ produced from the photo-irradiation of Rose Bengal. An aqueous mixture containing 50, 100, 150 or 200 μM UA and 10 μM Rose Bengal was irradiated by UVA light (1.12 mW/cm^2) for ~3 h until all the UA was consumed. Next, the UVA light was turned off and the reaction solution was left at room temperature for ~9 h. Concentrations of UA and products were analyzed by LC/TOFMS and HPLC as described below.

Oxidation of UA with $^1O_2$ produced from NEPO. Thermal decomposition of NEPO produces $^1O_2$. The purity of the NEPO was determined as 78% by the comparison of the UV absorption at 288 nm before and after the thermal decomposition of a methanolic solution of NEPO. Most of the NEPO was decomposed within 3 h at 35°C. A mixture of 50 or 100 μM UA and 8.0 mM NEPO in 50% aqueous methanol was incubated at 35°C for 3 or 12 h. Concentrations of UA and products were analyzed by LC/MS/MS and HPLC as described below.

Oxidation of UA with $^1O_2$ produced from H_2O_2 and NaClO or $ONOO^-$. UA (130 μM) was dissolved with 2.5 mM H_2O_2 in 100 mM phosphate buffer (pH 7.4) containing 100 μM diethylenetriamine-*N*,*N*,*N*′,*N*″,*N*″-pentaacetic acid (DTPA) for chelation of transition metal ions. Next, 33 μl of 182 mM aqueous NaClO solution was added into 20 ml of the well-stirred reaction mixture at a constant rate (2 μM NaClO/min) using a syringe pump (Harvard Apparatus, Holliston, MA) over 2.5 h.

A methanolic SIN-1 solution (100 mM) or an aqueous $ONOO^-$ solution (330 mM) was added to 100 mM phosphate buffer (pH 7.4) containing 150 μM UA, 2.5 mM H_2O_2, and 100 μM DTPA and incubated at room temperature for 3 h.

In the absence of H_2O_2, the oxidation of UA by NaClO or $ONOO^-$ was carried out at room temperature for 3 h. Concentrations of UA and products were determined by HPLC as described below.

UA oxidation by peroxyl radicals from 2',2-azobis(2-amidinopropane) dihydrochloride (AAPH). A mixture of 150 μM UA and 10 mM AAPH in phosphate buffer solution (pH 7.4) containing 100 μM DTPA was incubated at 37°C for 3 h. Concentrations of UA and products were determined by HPLC as described below.

Hydrolysis of PA to OUA. Phosphate buffers at pH 4.0 to 8.5 were prepared by adding 1 M NaOH or 1 M H_3PO_4 to the buffer solutions. Each 500 μM PA solution at various pHs was incubated under aerobic conditions at room temperature for 6 h. Concentrations of UA and OUA were determined by HPLC as described below.

PA detection on human skin surface. Five healthy volunteers participated in this study after giving informed consent. Skin surface UA and OUA were collected from their forearms before and after exposure to sunlight for 2 h. The collection procedure was as follows. Five glass tubes containing 1.0 ml of methanol were prepared. The open end of each tube (ø 20 mm) was pressed tightly against the skin at different locations on the forearm and then rotated carefully to allow the methanol to contact the skin for 1 min. The extracts were combined and the solvent removed using a nitrogen gas flow. The residue was re-dissolved into methanol and analyzed using LC/MS/MS.

HPLC analysis. The amounts of UA and its oxidative metabolites, PA, OUA, and AL, were determined by monitoring the absorption at 210 nm using a reversed-phase HPLC. The mobile phase was aqueous ammonium acetate (40 mM) and delivered at a rate of 1.0 ml/min. An ODS column (Tosoh, Tokyo, Japan; 5 μm, 4.6 mm × 250 mm) or a Develosil C30-UG (Nomura Chemical Co., Ltd., Tokyo, Japan; 5 μm, 250 mm × 4.6 mm) was used for separation. Retention times for UA, PA, OUA and AL were 7.8, 3.2, 11.0 and 2.5 min, respectively, using the ODS column, and 14.0, 7.0, 11.5 and 4.1 min, respectively, using the C-30 column.

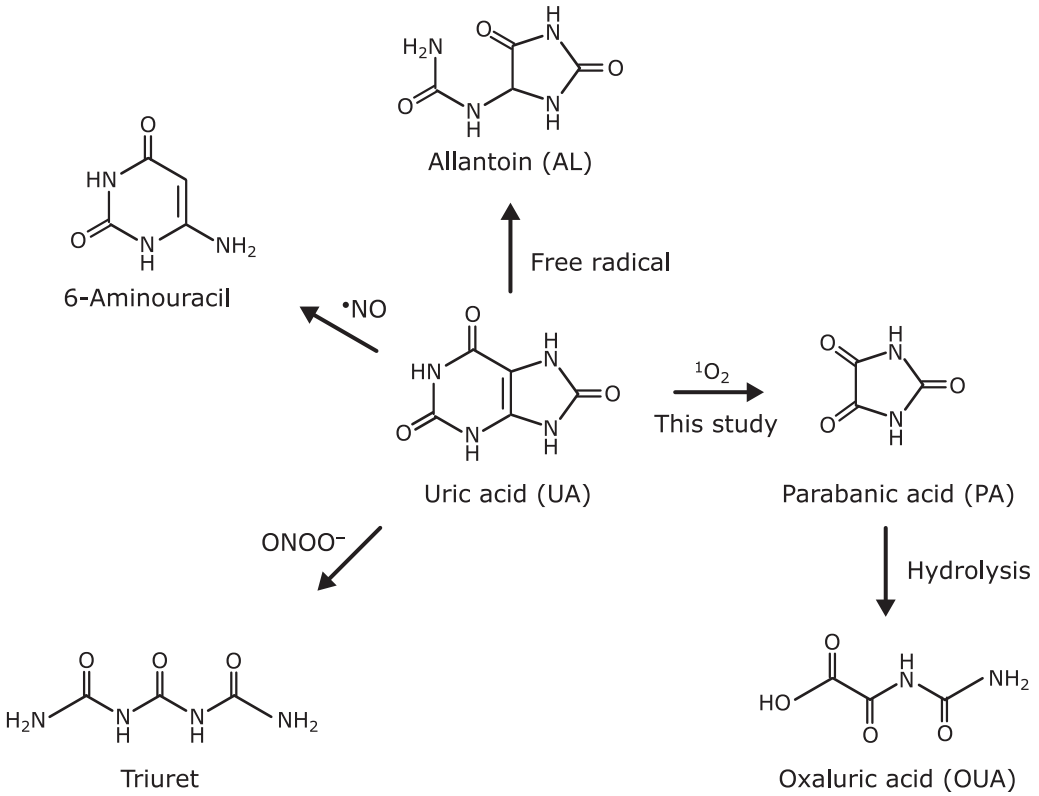

Fig. 1. Reported oxidation products of UA induced by reactive oxygen species: AL is produced by free radical-induced oxidation; triuret by $ONOO^-$; 6-aminouracil by •NO; and PA by $^1O_2$ (this study).

doi: 10.3164/jcbn.17-24

LC/TOFMS analysis. To obtain accurate mass-to-charge ratios (*m/z*) of UA oxidative metabolites, HPLC combined with TOFMS (JMS-T100LC, JEOL Ltd., Tokyo, Japan) was used. Negative ionization was performed at an ionization potential of –2,000 V. The optimized applied voltages to the ring lens, outer orifice, inner orifice, and ion guide were –5 V, –10 V, –5 V and –500 V respectively. To obtain accurate *m/z* values, trifluoroacetic acid (TFA) was used as an internal standard for *m/z* calibration.

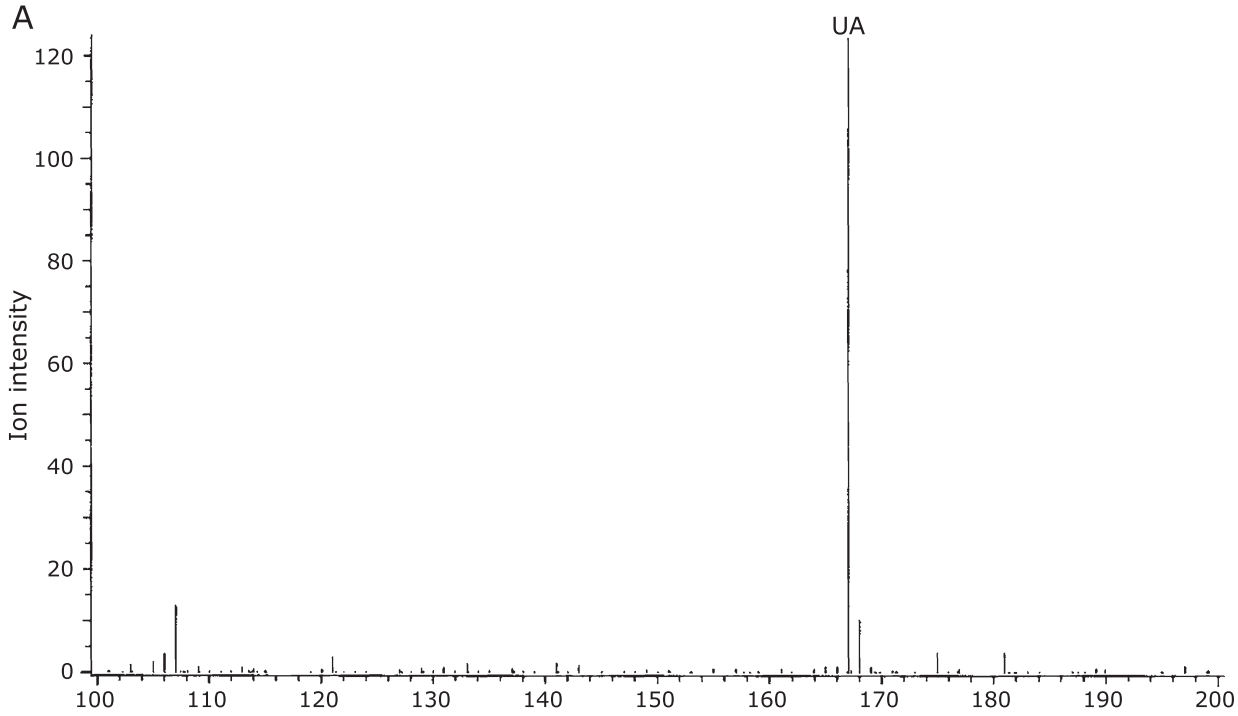

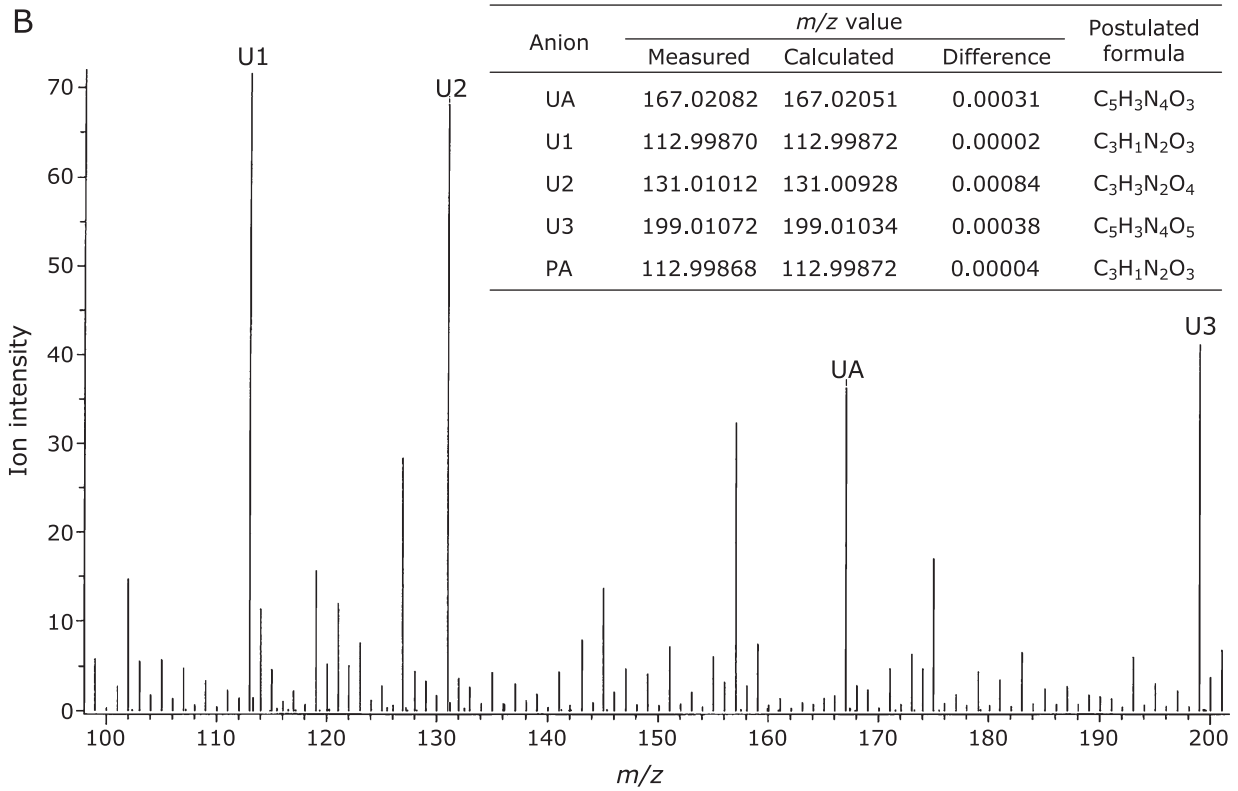

Anion	*m/z* value			Postulated formula
	Measured	Calculated	Difference	
UA	167.02082	167.02051	0.00031	$C_5H_3N_4O_3$
U1	112.99870	112.99872	0.00002	$C_3H_1N_2O_3$
U2	131.01012	131.00928	0.00084	$C_3H_3N_2O_4$
U3	199.01072	199.01034	0.00038	$C_5H_3N_4O_5$
PA	112.99868	112.99872	0.00004	$C_3H_1N_2O_3$

Fig. 2. MS spectra of 200 μM UA (A) before and (B) after 60-min photooxidation induced by UVA irradiation (1.12 mW/cm^2) using 10 μM Rose Bengal as a sensitizer. The TOFMS analysis was conducted in negative ESI mode with an ionization potential of –2,000 V. The measured *m/z* values were corrected using TFA as an internal standard. The chemical formula of PA and its candidates of U1, U2 and U3 are shown in the insert table with measured and calculated *m/z* values.

LC/MS/MS analysis. An LC/MS/MS system (LCMS-8040, Shimadzu, Kyoto, Japan) was used to determine the amounts of PA and OUA at the picomole level. Aqueous formic acid (0.2 ml/min, pH 3.5) was used as the mobile phase with a Develosil C30-UG column (Nomura Chemical Co., Ltd., Tokyo, Japan; 5 μm, 250 mm × 2.0 mm). Negative ionization was performed at −3.2 kV using an electrospray probe. For identification and quantification of each compound, multiple reaction monitoring (MRM) measurements were obtained. Optimized combinations of product and precursor ions for PA and OUA were determined as −42/−113 and −59/−131 respectively. Chromatographic retention times for PA and OUA were 6.0 and 10.5 min, respectively.

Results and Discussion

Identification of $^1O_2$-induced oxidation products of UA. $^1O_2$ was produced from UVA irradiated 10 μM Rose Bengal. Figure 2 shows the changes in the MS spectra in the presence of 200 μM UA before (Fig. 2A) and 60 min after irradiation (Fig. 2B), as determined by negative electrospray ionization (ESI) mode TOFMS. The UA concentration was reduced to 35% and three unidentified anions, U1, U2 and U3, appeared in the MS spectrum after 60 min. These products were not seen in the absence of UA, suggesting they were derived from UA. The *m/z* value of U1 was determined to be −112.99870 using TFA as an internal standard, and its chemical formula was postulated to be $C_3HN_2O_3$. This chemical formula is identical with that of PA and the *m/z* value of authentic PA is −112.99868. Furthermore, the retention times of U1 and authentic PA were identical (data not shown). We therefore concluded that U1 is PA.

The chemical formula of U2 was also determined to be $C_3H_4N_2O_4$, by its *m/z* value. This chemical formula is identical with OUA, a hydrolysate of PA. The retention times and MS spectra of U2 and authentic OUA were identical (data not shown), indicating that U2 is OUA. U3 ($C_5H_4N_4O_5$) was shown to be an O_2 adduct of UA.

Hydrolysis of PA to OUA. The effect of pH on the stability of aqueous PA was examined. The rates of PA hydrolysis and OUA formation increased with increasing pH (Fig. 3). The formation of OUA was stoichiometric with the decomposition of PA. The OUA formed was stable in solution at all pHs (4–8.5) for at least 1 week (data not shown).

The above results indicate that the $^1O_2$-induced oxidation products of UA are PA and its hydrolysate OUA. We next examined whether this is true in other $^1O_2$ formation systems such as thermal decomposition of NEPO and H_2O_2 plus ClO^- or $ONOO^-$.

Time course changes in PA and OUA levels during the oxidation of UA in various $^1O_2$ production systems. First, we employed NEPO which gives $^1O_2$ by its thermal decomposition. Figure 4A shows time course changes in UA, PA and OUA when 100 μM UA and 8 mM NEPO were incubated in methanol/water (50/50) at 35°C for 3 h. The major product was PA with a little OUA. The total yield of PA and OUA to consumed UA was 66.6%. When 1 mM NaN_3, an $^1O_2$ scavenger, was added to the reaction system, the rates of UA consumption and PA formation were reduced (Fig. 4B). The total yield of PA and OUA was also reduced to 13.2%, indicating that $^1O_2$ is a key oxidant of UA. All the NEPO was decomposed within 4 h at 35°C. However we incubated the reaction solution for another 9 h and found an increase of PA and OUA formation (Table 1), indicating that intermediates such as U3 slowly decomposed to PA. Therefore, the total yield of PA and OUA increased to 99.1%, indicating that PA and OUA are the exclusive products of $^1O_2$-induced oxidation of UA. This was also the case in the UVA-irradiated Rose Bengal system (Fig. 5A and Table 1).

Since all NEPO was converted to $^1O_2$, we knew how much $^1O_2$ was produced. We could then calculate the ratio of the amount of UA consumed to the total amount of $^1O_2$ generated in the system. This ratio was 1/370 or 1/180, respectively, when 50 or 100 μM UA was oxidized (Table 1), indicating that $^1O_2$ was predominantly quenched physically by UA or solvents. In fact, the rate constant for the quenching of $^1O_2$ by UA was reported to be $3.6 \times 10^8\ M^{-1}\cdot s^{-1}$,[23] while the rate constant for the reaction of $^1O_2$ with UA was determined to be $2.3 \times 10^6\ M^{-1}\cdot s^{-1}$.[24]

The mechanism of PA formation remains unclear. The isolated U3 decomposed under neutral conditions to form PA (data not shown), suggesting that U3 is a direct precursor of PA formation. Identification of U3 is under investigation.

Hydrogen peroxide is known to be converted to $^1O_2$ by the reaction with ClO^-.[20,21] To confirm this, we incubated aqueous UA in the presence of H_2O_2 with ClO^-. Figure 5B shows the time course changes in UA, PA and OUA when 130 μM UA was incubated with 2.5 mM H_2O_2 and NaClO. NaClO was added at a rate of 2 μM/min from 30 min. Thereafter, UA was decreased and PA was increased. The total yield of PA and OUA reached 56.1% for 2.5 h oxidation. In the absence of H_2O_2, the rate of UA consumption was slower and a little formation of PA and OUA (1.3% yield) was observed (Table 1 and Fig. 5E). These results suggest that ClO^--induced oxidation of UA only produced slight PA and OUA and ClO^- converted H_2O_2 to $^1O_2$.

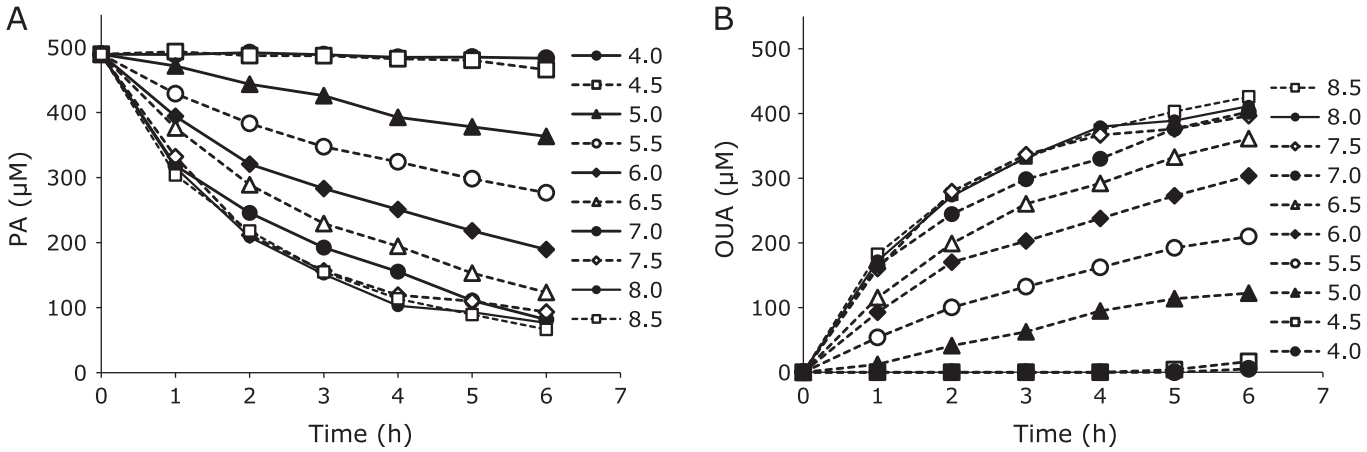

Fig. 3. Hydrolysis of (A) PA to (B) OUA at room temperature at various pHs (4.0–8.5).

doi: 10.3164/jcbn.17-24

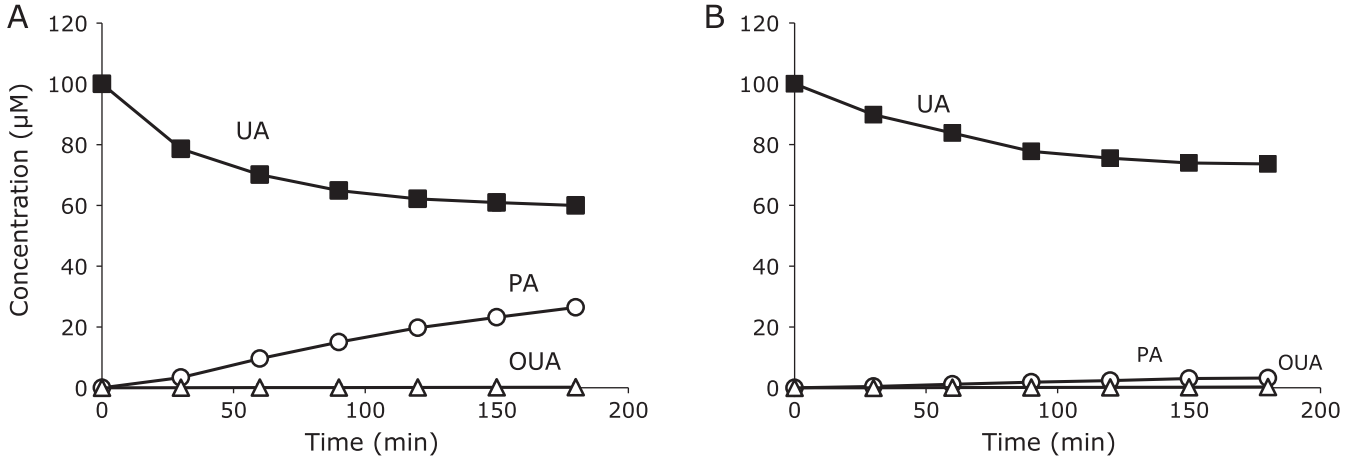

Fig. 4. Oxidation of 100 μM UA (■) in methanol/H_2O = 50/50 by $^1O_2$ derived from 8.0 mM NEPO at 35°C and the formation of PA (○) and OUA (△) in the absence (A) and in the presence (B) of 1.0 mM NaN_3. All data are expressed as mean ± SD (n = 3).

Table 1. Formation of PA and OUA and their yields during UA oxidation induced by different types of ROS [μM, mean ± SD (n = 3)]

ROS	$[UA]_0$	Time (h)	−Δ [UA]	[PA]	[OUA]	[PA] + [OUA]	Yield (%)
$^1O_2$ from 8.0 mM NEPO	50	12	21.3 ± 1.3	20.4 ± 1.3	0.29 ± 0.07	20.7 ± 1.4	97.0 ± 2.0
$^1O_2$ from 8.0 mM NEPO	100	3	40.0 ± 2.2	26.4 ± 0.9	0.18 ± 0.01	26.6 ± 0.9	66.6 ± 1.3
$^1O_2$ from 8.0 mM NEPO + 1.0 mM NaN_3	100	3	26.4 ± 0.4	3.21 ± 0.04	0.25 ± 0.01	3.5 ± 0.04	13.2 ± 0.2
$^1O_2$ from 8.0 mM NEPO	100	12	44.6 ± 1.1	42.4 ± 0.8	0.57 ± 0.13	44.2 ± 1.2	99.1 ± 0.3
$^1O_2$ from UVA-irradiated Rose Bengal	50	12	50	7.2 ± 0.2	41.6 ± 0.4	48.8 ± 0.4	97.6 ± 0.8
$^1O_2$ from UVA-irradiated Rose Bengal	100	12	100	18.3 ± 0.4	78.6 ± 0.5	96.9 ± 0.2	96.9 ± 0.2
$^1O_2$ from UVA-irradiated Rose Bengal	150	12	150	33.1 ± 0.2	109.4 ± 0.1	142.5 ± 0.3	95.0 ± 0.2
$^1O_2$ from UVA-irradiated Rose Bengal	200	2	157 ± 3.4	89.7 ± 3.6	1.9 ± 1.4	91.7 ± 5.0	58.4 ± 4.3
$^1O_2$ from UVA-irradiated Rose Bengal	200	12	200	55.7 ± 0.7	129.8 ± 0.1	185.4 ± 0.7	92.7 ± 0.4
$^1O_2$ from 2.5 mM H_2O_2 + 300 μM ClO^-	130	2.5	127 ± 0.5	70.9 ± 3.8	0.12 ± 0.003	71.0 ± 3.8	56.1 ± 3.3
$^1O_2$ from 2.5 mM H_2O_2 + $ONOO^-$ (1.0 mM SIN-1)	150	3	150	0.04 ± 0.01	56.2 ± 0.3	56.3 ± 0.3	37.0 ± 0.2
Peroxyl radicals from 10 mM AAPH	150	3	85.9 ± 4.2	1.2 ± 0.1	0.5 ± 0.1	1.7 ± 0.1	1.9 ± 0.1
ClO^- (360 μM)	260	3	243 ± 9.9	1.6 ± 0.2	1.5 ± 0.2	3.1 ± 0.2	1.3 ± 0.1
$ONOO^-$ (1.0 mM SIN-1)	200	3	132 ± 15	ND	ND	ND	0

ROS, reactive oxygen species; UA, uric acid; PA, parabanic acid; OUA, oxaluric acid; NEPO, 3-(1,4-dihydro-1,4-epidioxy-4-methyl-1-naphthyl)propionic acid; SIN-1, 3-(4-morpholinyl)sydnonimine, hydrochloride; ND, not detected.

Similarly, $ONOO^-$ converts H_2O_2 to $^1O_2$.[25,26] Figure 5C shows the time course changes in UA, PA and OUA when 150 μM UA was incubated with 2.5 mM H_2O_2 and 1.0 mM SIN-1, an $ONOO^-$ generator. The major product was OUA rather than PA because the pH of the reaction solution was ~8 which accelerated the hydrolysis of PA. The total yield of PA and OUA reached 37.0% for 3 h oxidation. In the absence of H_2O_2, the rate of UA consumption became slower and no formation of PA and OUA (0% yield) was observed (Table 1 and Fig. 5F). These results suggest that $ONOO^-$-induced oxidation of UA produced no PA and OUA and $ONOO^-$ converted H_2O_2 to $^1O_2$. It is noteworthy that similar results were obtained when synthetic $ONOO^-$ was used instead of SIN-1 (data not shown).

Oxidation of UA induced by peroxyl radical, ClO^-, or $ONOO^-$. Thermal decomposition of AAPH produces two *tert*-carbon-centered radicals which are immediately converted to two *tert*-peroxyl radicals. Peroxyl radical-induced oxidation of aqueous UA resulted in UA decay and AL formation (Fig. 5D). The total yield of PA and OUA was only 1.9% but this was significant. This may suggest that a small amount of $^1O_2$ was formed by the termination of two *tert*-peroxyl radicals,[27] and/or the Russell-reaction of two methylperoxyl radicals formed by β-scission of *tert*-alkoxyl radical occurred.[27–29] However, this requires further investigation.

As shown before, the total yield of PA and OUA in ClO^- and $ONOO^-$-induced oxidation of UA was below 2%. Therefore, we concluded that PA is the $^1O_2$ specific oxidation product of uric acid. We next tried to detect PA in biological samples.

Detection of PA on human skin surface. Human skin surface was selected as a candidate of PA detection since UA is present there and the level of squalene hydroperoxide ($^1O_2$ oxidation product of squalene) increases after sunlight exposure.[30] Methanol extracts of human skin were analyzed by LC/MS/MS. The analysis revealed the presence of UA and PA in skin lavage samples, but no OUA was detected. It is interesting that the PA and UA levels increased upon sunlight exposure (Table 2). The latter should be a protective response of human skin surface against photooxidation.

We are currently applying this method to human plasma samples. We believe our method is useful to determine the importance of $^1O_2$ and its significance in many diseases under oxidative stress.

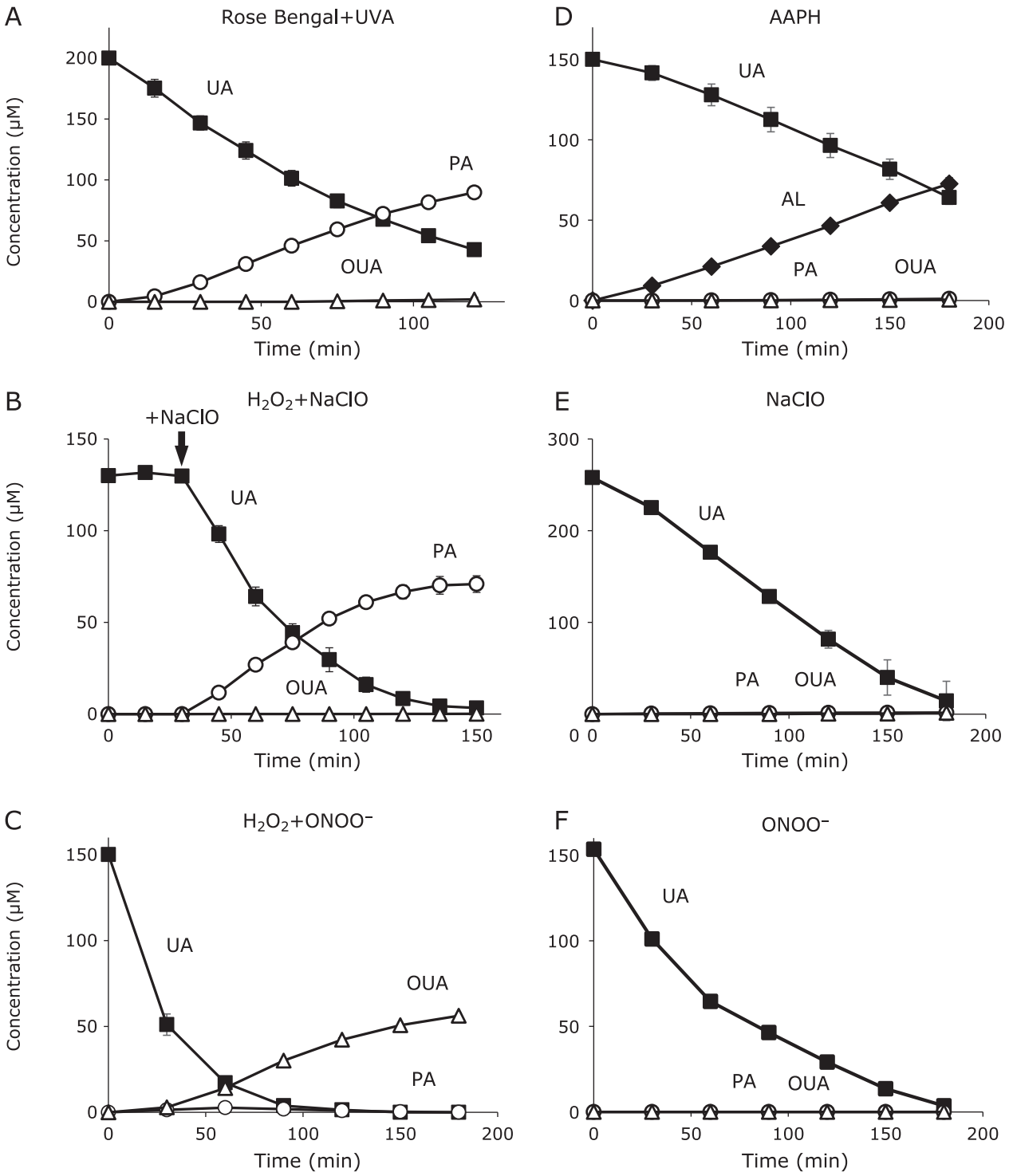

Fig. 5. Oxidation of UA (■) and the formation of PA (○), OUA (△), and AL (◆). All data are expressed as mean ± SD (n = 3). (A) UVA-induced photooxidation of 200 μM aqueous UA in the presence of 10 μM Rose Bengal. (B) Oxidation of 130 μM UA by $^1O_2$ produced from 2.5 mM H_2O_2 and 300 μM NaClO in 100 mM phosphate buffer (pH 7.4) at room temperature. Constant addition of NaClO (2 μM/min) was started at 30 min. (C) Oxidation of 150 μM UA by $^1O_2$ produced from 2.5 mM H_2O_2 and 1.0 mM SIN-1 ($ONOO^-$ generator) in 100 mM phosphate buffer (pH 7.4) at room temperature. (D) Oxidation of 150 μM aqueous UA with peroxyl radicals produced from 10 mM AAPH at 37°C. (E) Oxidation of 260 μM UA with 360 μM NaClO in 100 mM phosphate buffer (pH 7.4) at room temperature. The addition of NaClO was kept constant (2 μM/min). (F) Oxidation of 190 μM UA by 1.0 mM SIN-1 in 100 mM phosphate buffer (pH 7.4) at room temperature.

Conclusions

We identified PA as the $^1O_2$ specific oxidation product of UA. PA is slowly hydrolyzed to OUA under neutral conditions. Therefore, PA and OUA can serve as novel $^1O_2$ markers *in vivo*. We detected PA on human skin surface and its level increased upon sunlight exposure, indicating that sunlight exposure induced the formation of $^1O_2$ on human skin surface.

doi: 10.3164/jcbn.17-24

Table 2. PA formation and UA secretion on human forearm skin surface exposed to sunlight for 2 h

PA (pmol/cm²)			UA (pmol/cm²)		
Before exposure	After exposure	After/Before	Before exposure	After exposure	After/Before
0.020 ± 0.010	0.065 ± 0.040*	3.1 ± 1.2	13.9 ± 15.1	46.2 ± 30.8	4.8 ± 4.2

PA, parabanic acid; UA, uric acid; Each value represents mean ± SD (n = 5); *p<0.05.

Abbreviations

AAPH 2',2-azobis(2-amidinopropane) dihydrochloride
AL allantoin
DTPA diethylenetriamine-*N*,*N*,*N*′,*N*″,*N*″-pentaacetic acid
ESI electrospray ionization
NEPO 3-(1,4-dihydro-1,4-epidioxy-4-methyl-1-naphthyl) propionic acid
OUA oxaluric acid
PA parabanic acid
ROS reactive oxygen species
SIN-1 3-(4-morpholinyl)sydnonimine, hydrochloride
TFA trifluoroacetic acid
TOFMS time-of-flight mass spectrometry
UA uric acid

Conflict of Interest

No potential conflicts of interest were disclosed.

References

1 Flynn TP, Allen DW, Johnson GJ, White JG. Oxidant damage of the lipids and proteins of the erythrocyte membranes in unstable hemoglobin disease. Evidence for the role of lipid peroxidation. *J Clin Invest* 1983; **71**: 1215–1223.
2 Kasai H, Okada Y, Nishimura S, Rao MS, Reddy JK. Formation of 8-hydroxydeoxyguanosine in liver DNA of rats following long-term exposure to a peroxisome proliferator. *Cancer Res* 1989; **49**: 2603–2605.
3 Dukan S, Farewell A, Ballesteros M, Taddei F, Radman M, Nyström T. Protein oxidation in response to increased transcriptional or translational errors. *Proc Natl Acad Sci U S A* 2000; **97**: 5746–5749.
4 Ames BN, Gold LS, Willett WC. The causes and prevention of cancer. *Proc Natl Acad Sci U S A* 1995; **92**: 5258–5265.
5 Odegaard AO, Jacobs DR Jr, Sanchez OA, Goff DC Jr, Reiner AP, Gross MD. Oxidative stress, inflammation, endothelial dysfunction and incidence of type 2 diabetes. *Cardiovasc Diabetol* 2016; **15**: 51.
6 Smith MA, Richey Harris PL, Sayre LM, Beckman JS, Perry G. Widespread peroxynitrite-mediated damage in Alzheimer's disease. *J Neurosci* 1997; **17**: 2653–2657.
7 Jaeschke H, Smith CV, Mitchell JR. Reactive oxygen species during ischemia-reflow injury in isolated perfused rat liver. *J Clin Invest* 1988; **81**: 1240–1246.
8 Yamamoto Y, Yamashita S. Plasma ubiquinone to ubiquinol ratio in patients with hepatitis, cirrhosis, and hepatoma, and in patients treated with percutaneous transluminal coronary reperfusion. *Biofactors* 1999; **9**: 241–246.
9 Ames BN, Cathcart R, Schwiers E, Hochstein P. Uric acid provides an antioxidant defense in humans against oxidant- and radical-caused aging and cancer: a hypothesis. *Proc Natl Acad Sci U S A* 1981; **78**: 6858–6862.
10 Hooper DC, Spitsin S, Kean RB, *et al*. Uric acid, a natural scavenger of peroxynitrite, in experimental allergic encephalomyelitis and multiple sclerosis. *Proc Natl Acad Sci U S A* 1997; **95**: 675–680.
11 Grootveld M, Halliwell B, Moorhouse CP. Action of uric acid, allopurinol and oxypurinol on the myeloperoxidase-derived oxidant hypochlorous acid. *Free Radic Res Commun* 1987; **4**: 69–76.
12 Kaur H, Halliwell B. Action of biologically-relevant oxidizing species upon uric acid. Identification of uric acid oxidation products. *Chem Biol Interact* 1990; **73**: 235–247.
13 Robinson KM, Morré JT, Beckman JS. Triuret: a novel product of peroxynitrite-mediated oxidation of urate. *Arch Biochem Biophys* 2004; **423**: 213–217.
14 Gersch C, Palii SP, Kim KM, Angerhofer A, Johnson RJ, Henderson GN. Inactivation of nitric oxide by uric acid. *Nucleosides Nucleotides Nucleic Acids* 2008; **27**: 967–978.
15 Nakano M, Kambayashi Y, Tatsuzawa H, Komiyama T, Fujimori K. Useful $^1O_2$ ($^1\Delta_g$) generator, 3-(4'-methyl-1'-naphthyl)-propionic acid, 1',4'-endoperoxide (NEPO), for dioxygenation of squalene (a skin surface lipid) in an organic solvent and bacterial killing in aqueous medium. *FEBS Lett* 1998; **432**: 9–12.
16 Wagner JR, Motchnik PA, Stocker R, Sies H, Ames BN. The oxidation of blood plasma and low density lipoprotein components by chemically generated singlet oxygen. *J Biol Chem* 1993; **268**: 18502–18506.
17 Morgan PE, Dean RT, Davies MJ. Inhibition of glyceraldehyde-3-phosphate dehydrogenase by peptide and protein peroxides generated by singlet oxygen attack. *Eur J Biochem* 2002; **269**: 1916–1925.
18 Ravanat JL, Di Mascio P, Martinez GR, Medeiros MH, Cadet J. Singlet oxygen induces oxidation of cellular DNA. *J Biol Chem* 2001; **276**: 40601–40604.
19 Morita A, Werfel T, Stege H, *et al*. Evidence that singlet oxygen-induced human T helper cell apoptosis is the basic mechanism of ultraviolet-A radiation phototherapy. *J Exp Med* 1997; **186**: 1763–1768.
20 Foote CS, Wexler S, Ando S, Higgins R. Chemistry of singlet oxygen. IV. Oxygenations with hypochlorite-hydrogen peroxide. *J Am Chem Soc* 1968; **90**: 975–981.
21 Held AM, Halko DJ, Hurst JK. Mechanisms of chlorine oxidation of hydrogen peroxide. *J Am Chem Soc* 1978; **100**: 5732–5740.
22 Kato Y, Ogino Y, Aoki T, Uchida K, Kawakishi S, Osawa T. Phenolic antioxidants prevent peroxynitrite-derived collagen modification *in vitro*. *J Agric Food Chem* 1997; **45**: 3004–3009.
23 Kanofsky JR. Quenching of singlet oxygen by human plasma. *Photochem Photobiol* 1990; **51**: 299–303.
24 Sueishi Y, Hori M, Ishikawa M, *et al*. Scavenging rate constants of hydrophilic antioxidants against multiple reactive oxygen species. *J Clin Biochem Nutr* 2014; **54**: 67–74.
25 Di Mascio, Bechara EJ, Medeiros MH, Briviba K, Sies H. Singlet molecular oxygen production in the reaction of peroxynitrite with hydrogen peroxide. *FEBS Lett* 1994; **355**: 287–289.
26 Di Mascio, Briviba K, Bechara EJ, Medeiros MH, Sies H. Reaction of peroxynitrite and hydrogen peroxide to produce singlet molecular oxygen ($^1\Delta_g$). *Methods Enzymol* 1996; **269**: 395–400.
27 Adam W, Kazakov DV, Kazakov VP. Singlet-oxygen chemiluminescence in peroxide reactions. *Chem Rev* 2005; **105**: 3371–3387.
28 Niu QJ, and Mendenhall. Yields of singlet molecular oxygen from peroxyl radical termination. *J Am Chem Soc* 1992; **114**: 165–172.
29 Kanofsky JR. Singlet oxygen production from the reactions of alkylperoxy radicals. Evidence from 1268-nm chemiluminescence. *J Org Chem* 1986; **51**: 3386–3388.
30 Hayashi N, Togawa K, Yanagisawa M, Hosogi J, Mimura D, Yamamoto Y. Effect of sunlight exposure and aging on skin surface lipids and urate. *Exp Dermatol* 2003; **12 Suppl 2**: 13–17.